Chapter 2

Ceramic material

2.1 Introduction

LTCCs evolved from HTCCs with the purpose of achieving low loss, high speed, and high density packaging, as higher material performance was required for ceramic material than that offered by the alumina used for HTCCs.

The major characteristic of LTCCs is that metals with low conductor resistance – Cu, Au, Ag and their alloys – are introduced into the ceramic as wiring, thus controlling conductor loss to a low level. As Table 2-1 shows, all the metals with low electrical resistance have a low melting point of around 1,000°C, and in order to allow cofiring with these metals, LTCC ceramics are required to be able to be fired at less than 1,000°C [1, 2].

Table 2-1 Electrical resistance and melting point of conductor metals.

Metal	Electrical resistance ($\mu\Omega \cdot$ cm)	Melting point (°C)
Cu	1.7	1,083
Au	2.3	1,063
Ag	1.6	960
Pd	10.3	1,552
Pt	10.6	1,769
Ni	6.9	1,455
W	5.5	3,410
Mo	5.8	2,610

Loss in high frequency circuits (the inverse number of value Q) is expressed as the relationship between dielectric loss and conductor loss ($1/Q_{total} = 1/Q_c + 1/Q_d$, Q_c: conductor Q value, Q_d: dielectric Q value), and the higher the

frequency becomes, the greater the effect of dielectric loss over conductor loss [3, 4]. For this reason, ceramics are required to have low dielectric loss.

In high frequency electronic components, several kinds of ceramic with different dielectric constants suited to the function of the circuit are desirable, embedded in a monolithic structure [5, 6]. For transmission lines, a low dielectric constant is effective for achieving high speed transmission of signals (as the propagation delay time of the signal T_{pd} is proportional to the square root of the dielectric constant). On the other hand, the wavelength λ_d of the electromagnetic waves in the dielectric is inversely proportional to the square root of the dielectric constant, so for making compact components such as filters and so on, a high dielectric constant is beneficial. Furthermore, it is necessary to introduce a high dielectric constant layer when forming decoupling functions.

In addition to these characteristics, and in order for components to maintain stable characteristics in their environment of use and for mounted components to retain reliable interconnections, it is important for the ceramics to have low thermal expansion (in particular, they should have a thermal expansion coefficient close to that of the silicon material of the mounted components). Additionally, they must have sufficient strength to withstand the stresses of product assembly during manufacture, as well as while in use. Furthermore, to efficiently release the heat generated by the LSI components mounted on it, ceramic material with high thermal conductivity is desirable.

In order to meet these requirements, composites of glass and ceramic, crystallized glass, composites of crystallized glass and ceramic, and liquid phase sintered ceramics are being developed, as shown in Table 1-1. As examples of liquid phase sintered ceramics, the compounds $BaSnB_2O_6$, $BaZrB_2O_6$, $Ba(Cu_{1/2}W_{1/2})O3$, Bi_2O_3-CuO type, $Pb(Cu_{1/2}W_{1/2})O3$, Bi_2O_3-Fe_2O_3 type, PbO-Sb_2O_3 type, PbO-V_2O_5 type and $Pb_5Ge_3O_{11}$ (melting point: 738°C), LiF, B_2O_3, Bi_2O_3, $Pb_5Ge_{2.4}Si_{0.6}O_{11}$ (melting point: 750°C), Pb_2SiO_4 (melting point: 750°C), $Li_2Bi_2O_5$ (melting point: 700°C) and so on are known as sintering additives that are added to ceramics at less than 10 wt% [7, 8, 9], but they are not typical of LTCCs.

This chapter focuses on the composites of glass and ceramic (especially alumina) that are most commonly used for LTCCs, and it describes the important points for development of materials that meet the requirements for the qualities of LTCCs – firing temperature, dielectric constant, dielectric loss, thermal expansion, strength, and thermal conductivity. This information can also be applied to high dielectric constant LTCCs in which alumina is replaced with perovskite oxides.

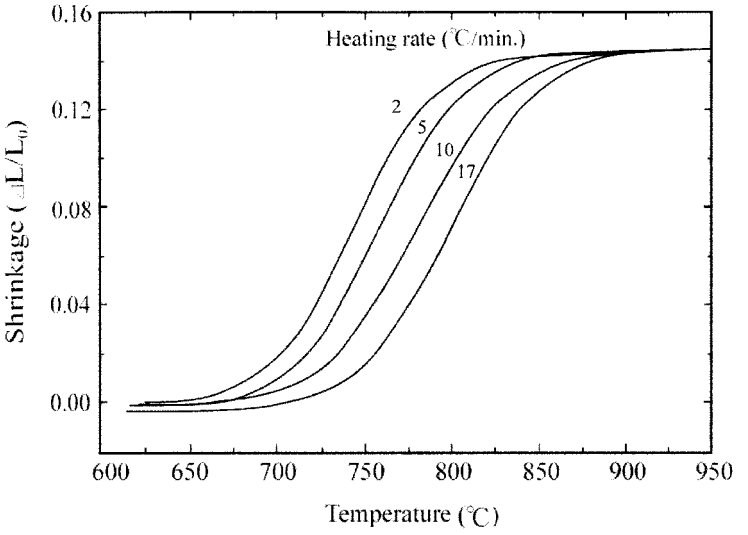

(a)

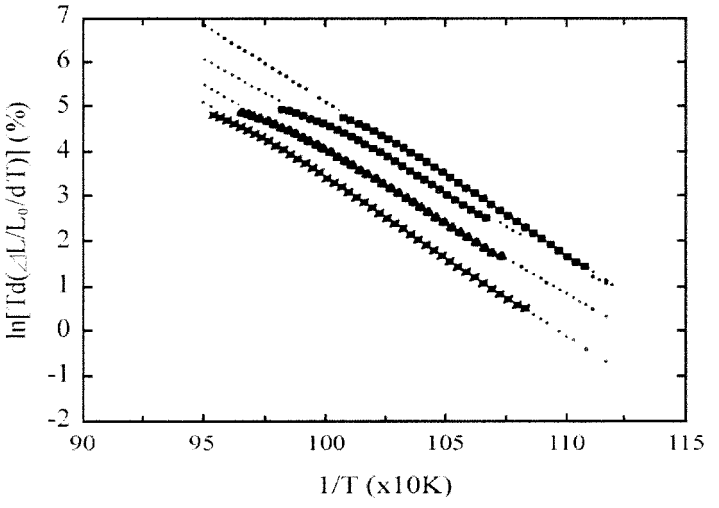

(b)

Figure 2-1 Curves for linear shrinkage rate (a) and curves for activation energy (b) in alumina/lead borosilicate glass composites at different programming rates [Ref. 10, 11].

2.2 Low temperature firing

The selection of glass materials is very important for sintering glass/ceramic composites, since the liquidation of the glass takes a dominant role in the viscous flow mechanism among the constituents. The ceramic particles in the composites dissolve slightly in the glass during sintering, although the

amount is very small and the ceramic is characterized by lack of grain growth. As shown in Figure 2-1, the shrinkage behavior in alumina and lead borosilicate glass composites was examined when the programming rate was changed, and the activation energy with regard to sintering behavior of these materials was calculated with formula (2-1). It is found that the liquidation of lead borosilicate glass is the rate-determining process of sintering [10, 11].

$$\ln[Td(\Delta L/L_0)/dT] = \ln(1/nK_0^{1/n})-1/n\ln\alpha-Q/nRT \qquad (2\text{-}1)$$

$\Delta L/L_0$: linear shrinkage rate, T: absolute temperature, α: programming rate, Q: sintering apparent activation energy, R: gas constant

When sintering composites of glass/ceramic, the liquidation of the glass is the key mechanism, where the glass penetrates the three dimensional mesh structure formed by the ceramic particles, facilitating the wetting of each ceramic particle surface with glass melt. Therefore in order to improve the sintered density of glass/ceramic composites, it is necessary to control the softening point of the glass material, as well as its volume and powder particle size to increase its fluidity [12, 13]. Furthermore, since the ceramic has the effect of an impediment hindering the flow of the glass, using ceramic with a large particle size and thus a small specific surface area is beneficial from the point of view of improving the sintered density.

As suggested above, factors arising from the characteristics of the glass play a very large role in low temperature firing. The following describes the basics of glass – fluidity, crystallization, foaming, and reactions – that need to be understood in order to achieve a high sintered density.

2.2.1 Fluidity of glass

As shown in Figure 2-2, a common structure for SiO_2 based amorphous glass is a network of Si-O modified with Na_2O, in which part of the network is segmented and non-bridging oxygen is formed [14]. The constituent oxides are broadly classified into oxides that make networks, modifier oxides that break the network, and intermediate oxides that can become oxides of either type. Since modifier oxides break the network, they lower the softening point of the glass and increase its fluidity. Table 2-2 details the effect on glass characteristics of the representative types of oxide that are ingredients of glass. Table 2-3 and Figure 2-3 show the composition of Corning's commercial glass and the temperature dependency of glass viscosity [15]. The softening point is the temperature at which viscosity is $10^{7.65}$ poise, and this is used as an index of glass fluidity. Using the above information, it is necessary to control the glass composition, and to choose glass with

appropriate fluidity that has the various characteristics required. In general, for glass/ceramic composite type LTCCs, borosilicate glass with a softening point of around 800°C is used.

Table 2-2 The effect of various glass ingredients on glass quality.

SiO_2	A substance that forms the network structures of glass. It has a high melting point and high viscosity. If the silica content in glass is high, the glass has a high transition temperature, low thermal expansion, and excellent chemical durability.
B_2O_3	A substance that forms network structures. Added to the network structure of quartz glass, it reduces viscosity without any negative impact on thermal expansion and chemical durability. It is one of the ingredients of heat-resisting glass and chemical glassware.
PbO	Although it does not form network structures, it can connect SiO_4 tetrahedrons. It is used for glass with a large dielectric constant, refractive index and specific resistance. As it is easily deoxidized, heat treatment in an atmosphere containing oxygen is necessary.
Na_2O	A modifier oxide. It lowers the softening point markedly. Furthermore, it increases the thermal expansion coefficient and ionic conductance. It also reduces chemical durability.
K_2O	A modifier oxide. Although it has the same effect as Na_2O, its K ion is comparatively large and therefore immobile.
Li_2O	A modifier oxide. Although it has the same effect as Na_2O, its Li ion is comparatively small and therefore very mobile. Furthermore, it crystallizes readily.
CaO	A modifier oxide. It prevents the migration of the alkali ion, and therefore the specific resistance and chemical durability of the alkali glass increases. Furthermore, the temperature range for thermal processing is narrowed down.
MgO/ ZnO	A modifier oxide. It has the same effect as CaO (its ionic radius is different).
BaO	This is used instead of PbO. It is cheaper than PbO, with a low degree of hazard.
Al_2O_3	An intermediate oxide. It differs in size from SiO_4 tetrahedrons, but in AlO_4 tetrahedrons it can connect to the network structure. It has the effect of controlling crystallization. Furthermore, since it increases viscosity, it makes melting difficult.

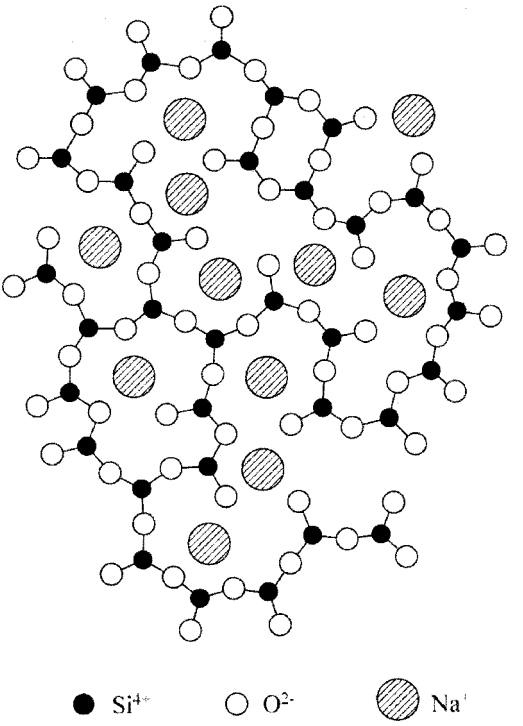

Figure 2-2 Structural schema of soda-silicate glass.

2.2.2 Crystallization of glass

In ceramic materials for LTCCs, there are cases where crystals are actively precipitated in the glass to achieve the required characteristics, and cases where precipitation of crystals that are not required in the glass is hindered. In either case, it is necessary to fully understand the occurrence of crystallization of glass, and to control crystal precipitation.

Table 2-3 Composition of commercial glass (wt%).

Glass coating (Corning)	SiO_2	B_2O_3	Al_2O_3	Na_2O	K_2O	MgO	CaO	PbO
FQ (Fused Silica)	99.8	-	-	-	-	-	-	-
Vycor 7900	96	3	1	-	-	-	-	-
Pyrex 7740	81	13	2	4	-	-	-	-
0080	72.6	0.8	1.7	15.2		3.6	4.6	-
0010	63	-	1	8	6	-	1	21
8870	35	-	-	-	7	-	-	58

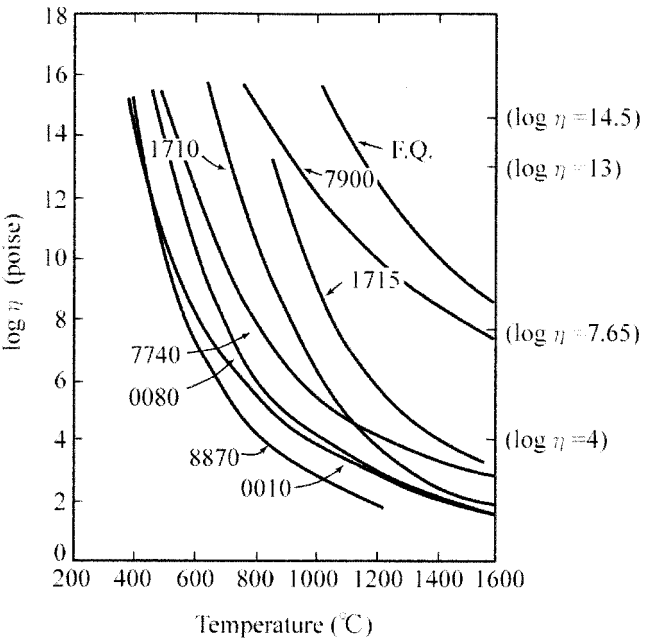

Figure 2-3 Temperature dependency of viscosity of commercial glass and various characteristic temperatures (Strain point: $10^{14.5}$ poise, Annealing point: 10^{13} poise, Softening point: $10^{7.65}$ poise, Working point: 10^{4} poise).

The formation of crystals in glass is broadly classified into two types, homogenous nucleation, and heterogeneous nucleation. Homogenous nucleation is where crystal nuclei are formed from a uniform glass phase to precipitate crystals. On the other hand, with heterogeneous nucleation, crystals are precipitated and grow from nuclei formed around elements for forming crystal nuclei introduced into the glass, as well as on the surface of foreign matter present in the glass, at the contact surfaces between the glass and its container such as a crucible, at the surface of the glass and so on. Crystallized glass with TiO_2, ZrO_2, metal ions and the like introduced into the base glass as the nucleation agent is representative of heterogeneous nucleation. With heterogeneous nucleation, differential thermal analysis (DTA) is generally used for analysis of the glass crystallization process and for examination of the crystal precipitation conditions. Figure 2-4 shows a typical DTA curve for glass [16]. The various kinds of characteristic temperature of glass can be estimated from the DTA results as shown in the Figure 2-4.

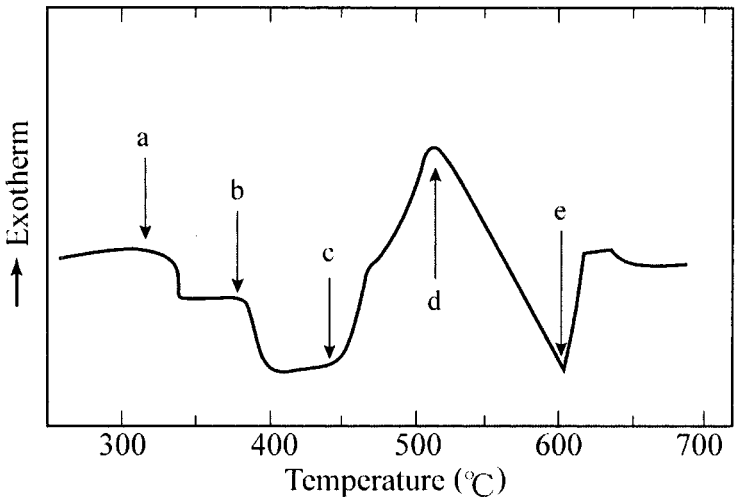

Figure 2-4 A typical DTA curve for glass (a: glass transition point, b: softening point, c: crystallization temperature, d: crystallization peak, e: melting temperature).

In order to control the microstructure of the crystals precipitated in the glass, it is necessary to understand nucleation temperature and nucleation speed, and the temperature for crystal growth and its speed. As in Figure 2-5, nucleation speed I and crystal growth speed U show a Gaussian distribution in relation to temperature, and at a specific temperature they reach their greatest speed. In the case of (a) in the figure, there is a big difference between the nucleation peak temperature and the crystal growth peak temperature, and as neither speed is high, the crystal nuclei formed in the glass disappear before the crystal growth temperature is reached so that vitrification is achieved easily. On the other hand, in the case of (b), I and U are close, and at the temperature range where many nuclei are generated, crystal growth speed is high so that crystals are formed readily in the glass matrix. In order to precipitate many crystals, a method is being tested whereby, after first performing heat treatment at the temperature where nucleation speed is high to generate many crystal nuclei, heat treatment is carried out with a heating schedule that maintains a high crystal growth speed T_u.

The nucleation temperature is decided by obtaining the exothermal peak temperature of crystallization measured by carrying out DTA analysis on each glass that is heat treated at various temperatures in advance (Figure 2-6 (a)), and by calculating the nucleation speed from the temperature difference with the crystallization temperature of glass that is not heat treated. Below

are the details of the calculation method for defining the relationship between the shift in the exothermal peak of crystallization when the pre-heating process is carried out, and nucleation speed.

The dynamics of the process in which nucleation and crystal growth occur together are expressed by the Johnson-Mehl-Avrami (JMA) equation.

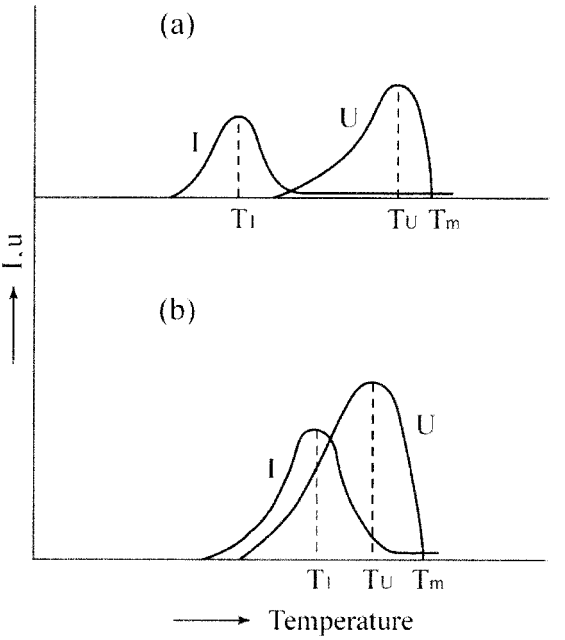

Figure 2-5 The temperature dependency of nucleation speed I and crystal growth speed U [(a): Vitrification occurs readily, (b) Crystals are formed readily] [Ref. 17].

$-\ln (1-x) = (kt)^n$ .... (2-2)
x: Volume fraction of crystals

$k = A\exp(-E/RT)$ .... (2-3)

A: Constant, E: Activation energy of crystal growth, $N = N_r + N_0/\alpha$, N_r is the number of crystal nuclei at the unit volume formed during heat treatment at nucleation temperature, and N_0/α is the number of crystal nuclei at the unit volume formed during the rise in temperature at speed α.

If the temperature rises at the constant programming rate α, since k changes in accordance with the temperature or time, equation (2-2) is expressed as equation (2-4).

$$-\ln (1-x) = \{1/\alpha \int k (T)\, dT\}^n \quad \ldots . \quad (2\text{-}4)$$

If equation (2-3) is substituted with (2-4), and the integral is found, and additionally the logarithm is taken, the following equation is obtained.

$$(1/n) \ln \{-\ln(1-x)\} = \ln (N_r+N_0/\alpha) - \ln\alpha - 1.052E/RT + \text{const.} \quad \ldots . \quad (2\text{-}5)$$

Assuming the temperature to be the DTA exothermal peak temperature T_p, for a non-treated sample, if $N_r = 0$, and if the DTA programming rate is fast, since $N_r / N_0 >> 1$with a heat treated sample, equation (2-5) can be rewritten as (2-6).

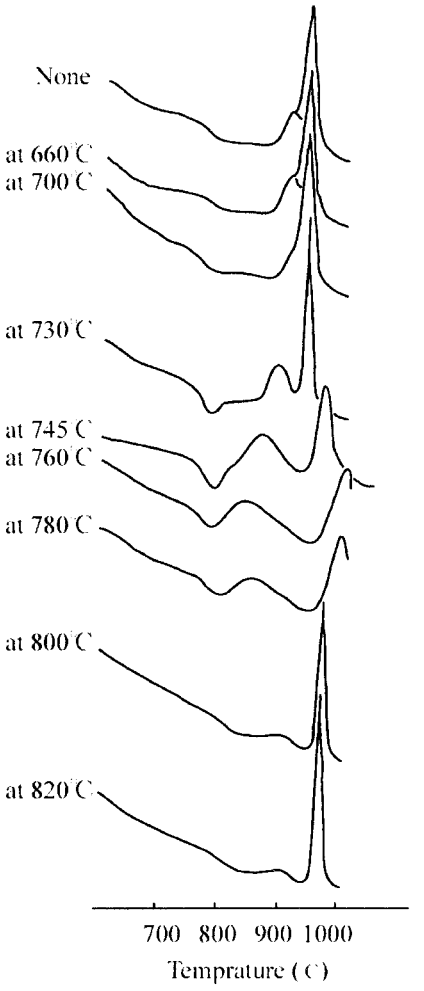

(a)

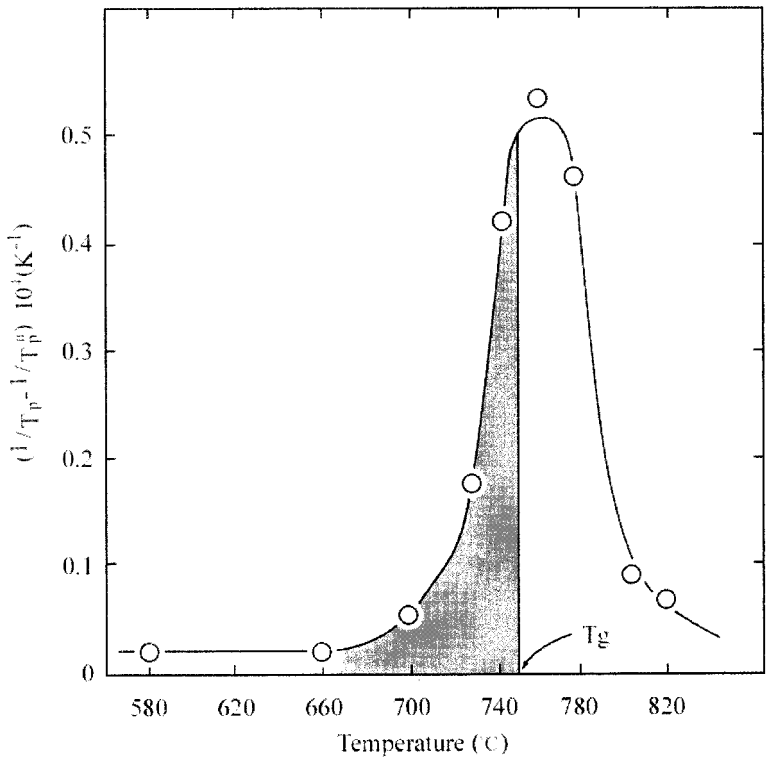

Figure 2-6 DTA curves for non heat treated glass and for glass that is heat treated at various temperatures for 8 hours (a), and the relationship between heat treatment temperature and nucleation speed (b) [Ref. 18].

$$\ln N_r = 1.05(E/R)[1/T_p - 1/T^0_p] + \text{const.} \quad \ldots . (2\text{-}6)$$

where, T^0_p is the exothermal peak temperature of the non-treated sample, while T_p is the DTA exothermal peak temperature of the sample after heat treatment at the nucleation temperature. If nucleation processing is carried out under isothermal conditions, then $N_r = It^b$. Here, I is nucleation speed, b is the constant, and t is the isothermal processing temperature. If the heat treatment time with a constant time of $N_r = It^b$ is replaced with (2-6), $\ln I = 1.052(E/R)[1/T_p - 1/T^0_p] + \text{const.}$

In this way, the heat treatment temperature dependency of nucleation speed can be expressed with variations of $[1/T_p - 1/T^0_p]$.

Furthermore, the crystal precipitation mechanism can be established by obtaining the amount of crystallization of the glass after testing with heat

treatment at various temperatures and times, plotting a graph in accordance with the JMA equation rewritten as $\ln\{\ln[1/(1-x)]\} = n\ln k + n\ln t$, and by finding the gradient of the graph n (refer to Figure 2-7, Table 2-4)[19, 20].

Crystal growth speed can be obtained by observing with an electron microscope the diameter of crystals precipitated in the glass after heat treatment at various temperatures and times, and plotting the results on a graph. In addition, by making an Arrhenius plot of crystal growth speed constants at each heat treatment temperature, it is possible to calculate the activation energy, and understand the rate determining steps of the reaction.

Table 2-4 The Avrami exponent for each form of crystal precipitation.

	Diffusion controlled	Interface controlled
3-dimension	1.5	3.0
2-dimension	1.0	2.0
1-dimension	0.5	1.0

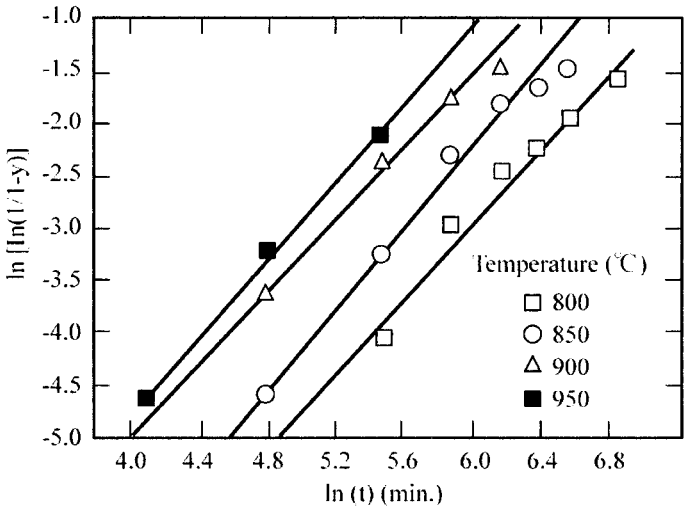

Figure 2-7 Plot of $\ln\{\ln[1/(1-x)]\}$ vs. $n\ln t$ for crystals precipitated in heat treated glass at 800°C to 950°C [Ref. 19, 20].

2.2.3 Foaming of glass

The formation of internal pores that is observed in LTCCs is sometimes caused by insufficient sintering, and sometimes by excessive sintering causing the occurrence of gas within the material. Figure 2-8 shows the microstructure in glass/alumina composite material. The pores from insufficient sintering observed in a sample fired at 800°C are angular (a), while the pore shape assumes a roundness (b) with increased firing temperature. Pores due to excessive sintering in material fired at 1,100°C appear spherical (c). There are two possible causes of these spherical pores. Cause (1): During sintering, the surface of the sample is sintered first, and after a well-sintered film is formed on the surface, the pores are formed when gas left inside the material or residues of organic binder are expelled at high temperature. Cause (2): The gas dissolved in the raw glass powder used in LTCCs is released at high temperature forming the pores.

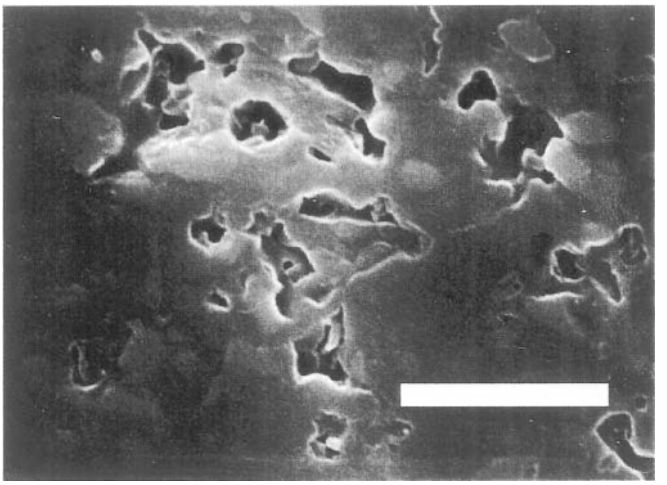

(a)

When glass melts, decomposition of the batch materials such as H_2BO_3, Na_2CO_3, Na_2SO_4, $NaNO_3$ and so on, releases large volumes of gas such as CO_2, SO_2 and the like[22, 23, 24, 25]. Most of this is released, however some of the gas forms bubbles and remains in the glass or dissolves inside the glass melt. In order to prevent foaming, it is important to examine the glass raw powder and to use raw materials containing little dissolved gas. (Caution is required as some commercially available glass powder contains ground up reject glass products.) In addition, reducing the time during the firing process at temperature ranges where gas occurs readily is effective in controlling the foaming of glass.

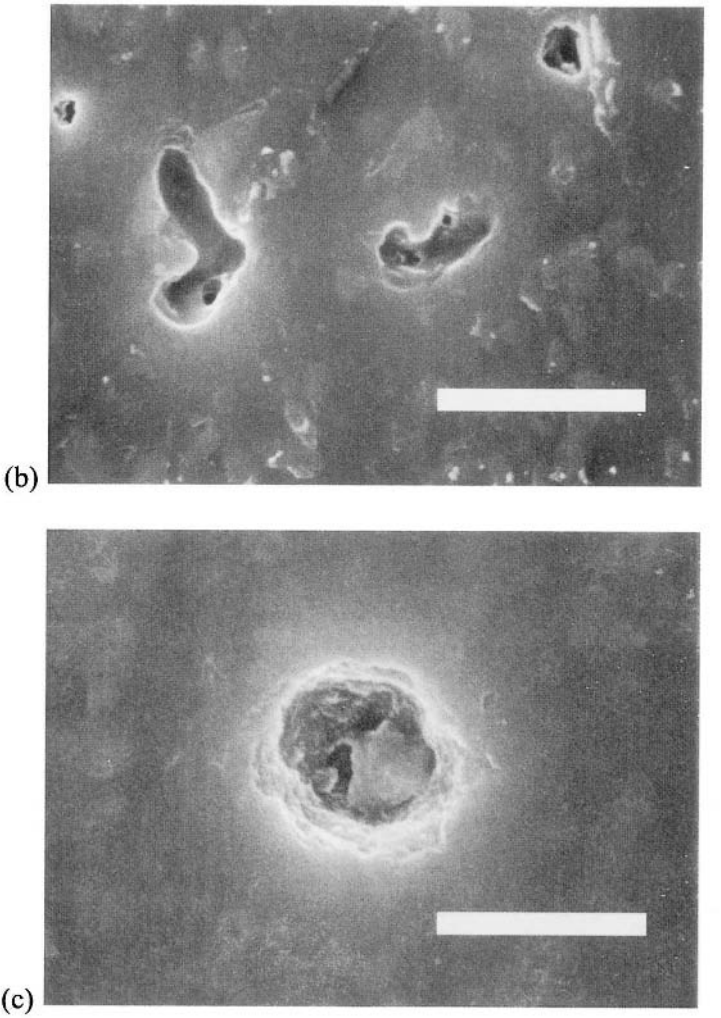

Figure 2-8 Microstructure of glass/alumina compound fired at various temperatures (a) 800°C, (b) 900°C, (c) 1,100°C [Bar = 5 μm] [Ref. 21].

Figure 2-9 shows the results of an investigation of changes in sintered density of glass/alumina composite at a lower temperature (900°C) than the final firing temperature of 1,000°C and when the retention time was changed. Sintered density falls abruptly with retention time. Although pores are not observed in the surface of the ceramic, many of the spherical pores noted above can be seen inside the ceramic like foam glass (Refer to Figure 2-10).

These results substantiate the view that gas originating inside the material forms the spherical cavities.

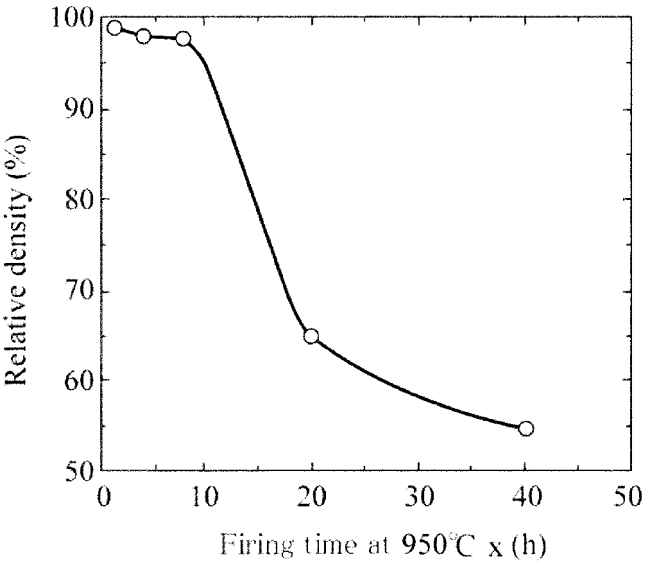

Figure 2-9 Sintered density of glass/alumina composite when 950°C retention time is changed.

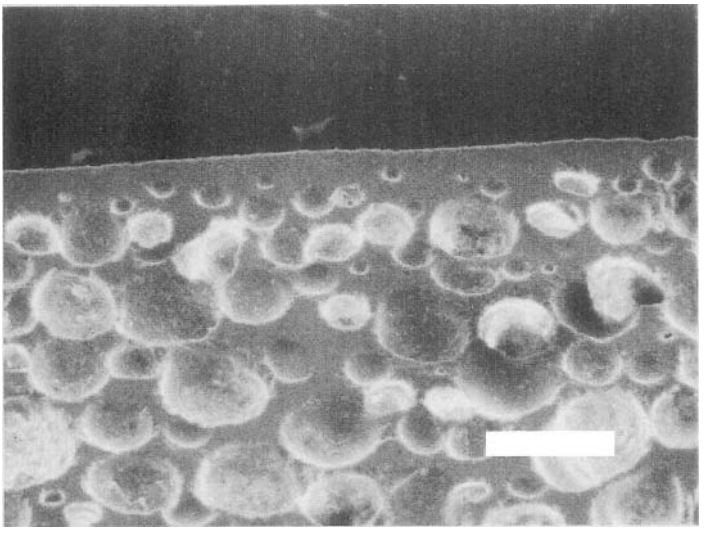

Figure 2-10 Microstructure of glass/alumina composite after heat treatment of 950°C for 20 h, and 1,000°C, for 5 h [Bar = 200 μm].

2.2.4 Reaction between glass and ceramic

In glass/alumina composites, the amount of alumina dissolved in the glass at firing is small, however this small amount suppresses crystallization of the glass, or in some cases promotes crystallization of the glass, playing an important role in improving or controlling different characteristics. For example, if borosilicate glass is heat treated as a simple substance, cristobalite crystals that have large thermal expansion are precipitated, and as well as making control of the thermal expansion of the LTCC impossible, they retard the density of the material [26]. However, when a composite is formed with alumina, precipitation of cristobalites can be suppressed, and a composite with a matrix of amorphous glass is obtained (refer to Figure 2-11) [27]. The suppression of cristobalite precipitation can be considered to be due to the alumina diffused into the glass from the alumina particles hindering the formation of crystal nuclei. Furthermore, with alumina/CaO-Al_2O_3-SiO_2-B_2O_3 glass, due to the alumina diffusing into the glass during firing, anorthites ($CaO \cdot Al_2O_3 \cdot 2SiO_2$) are precipitated in the glass resulting in mechanically stronger material [28]. With ceramics that aim for extreme precision while precipitating crystals during firing (including crystallized glass type LTCCs), since changes occur in the viscosity of the base glass phase along with crystal precipitation, it is necessary to rigorously control the parameters related to precision and shrinkage behavior such as the amount of crystal precipitation, crystal growth speed and so on, to fire with good repeatability. Furthermore, if warping occurs when firing the substrate, since the amount of remaining glass phase in the ceramic after firing is different from when firing, and the apparent softening point gets higher, unlike glass/ceramic composite types, the warping cannot easily be fixed by reheating and it will be necessary to control the processing conditions of the firing process more exactly. If LTCCs are used for circuit boards with fine wiring formed internally, since control of the wiring circuit dimensions is important, LTCCs of the amorphous glass and ceramic composite type with their simple sintering density process are beneficial from the point of view of shrinkage dimension control.

2.3 Dielectric characteristics

2.3.1 Dielectric constant

Since LTCCs are basically composite structures of glass and crystals, controlling their dielectric constant depends largely on the combination of constituent materials of the composite and its material composition (volume fraction of the constituent materials). In addition, the dielectric constant of

the constituent materials themselves (especially the glass material) has a big influence on the dielectric constant of the LTCC.

The dielectric constant of the materials themselves depends on the contribution of electrons or ions with regard to polarizability and their dipole orientation, and the following relationship obtains between polarizability Nα and relative permittivity ε per unit volume.

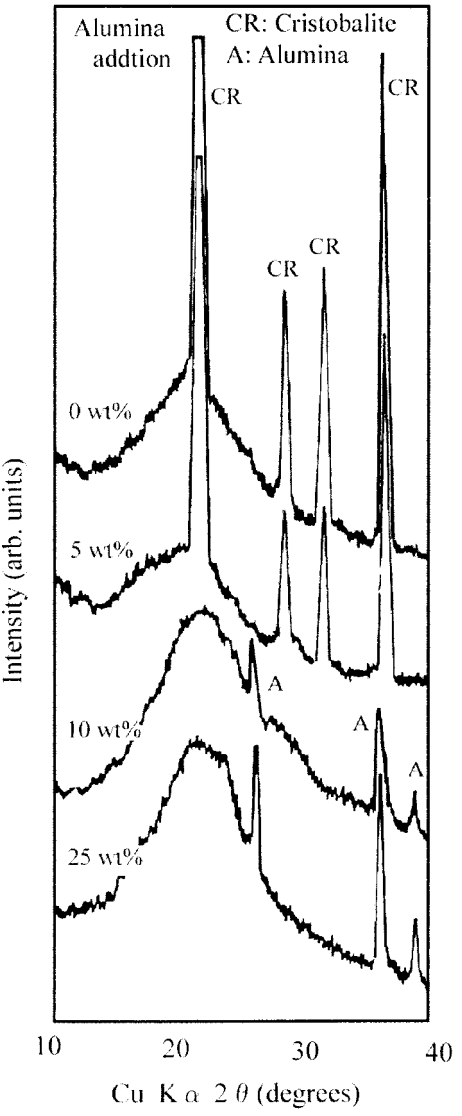

(a)

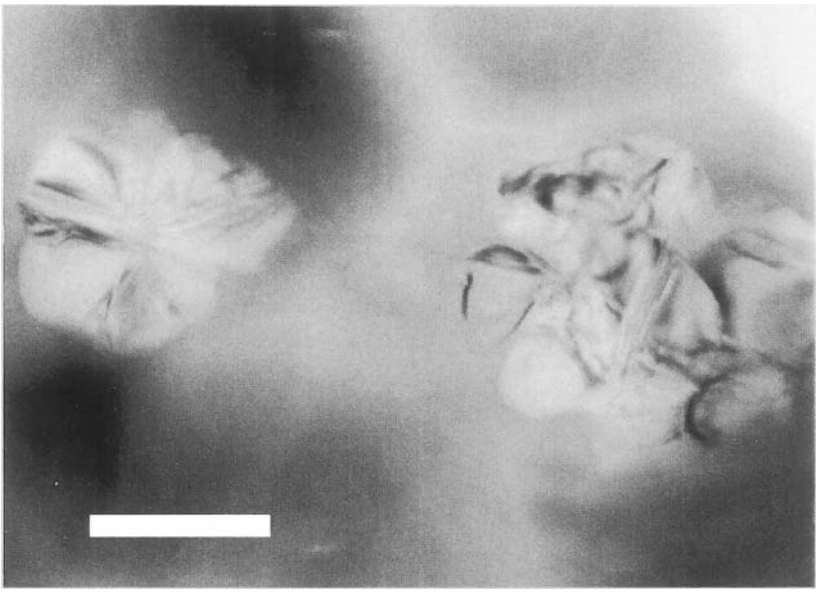

(b)

Figure 2-11 Results of X-ray diffraction of a glass/alumina composite when the amount of alumina added is changed (a), and cristobalite crystals precipitated in glass (b) [Bar = 1 μm].

$N\alpha/3\varepsilon_0 = (\varepsilon - 1)/(\varepsilon + 2)$
N: number of molecules per unit volume, α: polarizability, ε: relative permittivity,

The total polarizability of the dielectric is expressed as the sum of each polarizability feature.

$\alpha = \alpha_e + \alpha_i + \alpha_o + \alpha_s$
α_e: electronic polarization, α_i: ionic polarization, α_o: orientation polarization (dipole orientation), α_s: space charge polarization

Electronic polarization is the polarization that occurs due to the shift in center of gravity of the negative electron cloud with regard to the positive nucleus when a voltage is applied. In glass structures, with regard to the polarizability of electronic polarization, the bigger the ionic radius, the more negative the charge and the larger the number of charges as in $Ba^{2+} > Sr^{2+} > Ca^{2+} > Mg^{+}$, $O^{2-} > F^{-} > Na^{+} > Mg^{2+} > Al^{3+} > Si^{4+}$. Ionic polarization occurs when the positive ions in the glass relatively displace the anions in an electric field. Dipole orientation is associated with the dipoles formed of the modifier ion and non-bridging oxygen in the glass. When an electric field is applied to the glass, the modifier ions jump across the energy barrier formed

in the vicinity, and migrate in the direction of the electric field. If this change in the electric field is slow, the ions jump across a high energy barrier and migrate over a long distance, however, when the change in the electric field is fast, they jump across a low energy barrier, and do not migrate far. For this reason, it is a mechanism that occurs in low frequency regions. Dipole orientation is large in glass that includes alkali ions and OH - ions. Space charge polarization is polarization of migrated charges that accumulate in the vicinity of an electrode, grain boundaries within the material, and at the interfaces of dissimilar materials, without being neutralized. Seen from an external circuit, it appears as though capacity has increased. There are methods using a space charge, as a technology for achieving a high dielectric constant. As in Figure 2-12 by performing reduction processing and valency control of the basic dielectric particles themselves, they are made into semiconductors and their apparent dielectric constant is increased, and by giving the grain boundary part insulating properties, the withstand voltage is improved [29]. Another method involves, conversely, forming a material with high conductivity in a grain boundary phase, in a structure made up of dielectric particles with excellent insulation [30].

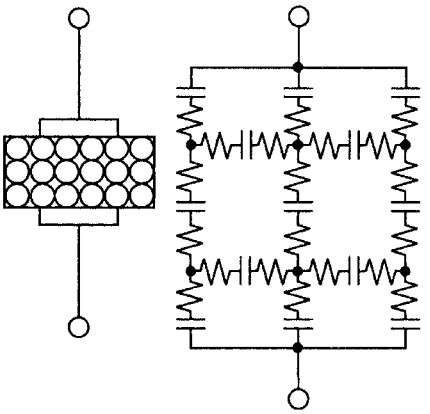

Figure 2-12 Microstructure model of a barrier layer type dielectric and its equivalent circuit.

In the composite, the dielectric constant is determined by the dielectric constant and volume fraction of the constituent material, and the complex form of the constituent material [31]. Table 2-5 shows the 4 different models of mixing rules for complex forms of the constituent materials. LTCC ceramics, being of the type with ceramic particles distributed in a glass matrix, fit the Maxwell model well. In order to achieve a lower dielectric

constant material, approaches are being made such as introducing relative permittivity 1 air phase as constituent material, for example with the use of hollow ceramic as a constituent material, forming a cavity phase during the firing process.

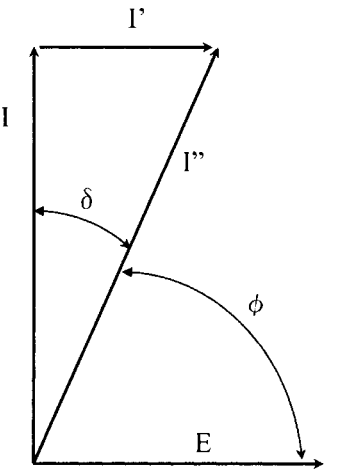

Figure 2-13 Phase relation of current and voltage.

Table 2-5 Mixture rules for effective dielectric constants of composites.

Composite type	Equation	Composite material Structure model
Parallel	$E = V_1\varepsilon_1 + V_2\varepsilon_2$	The composite constituent material is aligned parallel to the electric field
Series	$1/\varepsilon = V_1/\varepsilon_1 + V_2/\varepsilon_2$	The composite constituent material is aligned in series with the electric field
Logarithmic	$\ln\varepsilon = V_1\ln\varepsilon_1 + V_2\ln\varepsilon_2$	The composite constituent material is aligned randomly (empirical rule)
Maxwell	$\varepsilon = \{V_2\varepsilon_2 (2/3 + (\varepsilon_1/3\varepsilon_2)) + V_1\varepsilon_1\}/\{V_2(2/3 + (\varepsilon_1/3\varepsilon_2)) + V_1\}$	Spherical phases are distributed in the matrix (0-3 connectivity)

ε: dielectric constant of the composite, ε_1: dielectric constant of constituent material 1, ε_2: dielectric constant of constituent material 2, V_1: volume fraction of constituent material 1, V_2: volume fraction of constituent material 2

2.3.2 Dielectric loss

When an alternating voltage is applied to a capacitor that does not include a dielectric, power loss does not occur since the phase of the current is 90° in front of the voltage. However, if an electric field is applied to a capacitor that includes a dielectric, there is a phase shift in the electric displacement of the electric field, and some of the electric energy changes into heat in the dielectric. Dielectric loss is the amount of electric energy lost through conversion to heat in the dielectric when an electric field is applied. In Figure 2-13, the phase angle Φ of current I' is 90° smaller, and accompanies voltage E and the in-phase current component I''. Therefore, loss corresponding to I'' occurs. The size of this loss is expressed as tan δ = I''/I using δ as the complement of Φ.

In order to reduce the dielectric loss of LTCCs, similarly with the dielectric constant, it is effective to construct them of materials with low dielectric loss, use a large volume fraction of low dielectric loss materials, and to make the dielectric loss of each constituent material small. Among glass, a constituent material of LTCCs with large dielectric loss, the following four dielectric loss mechanisms are known. (1) Conduction loss through electric conductivity, (2) dipole relaxation loss from relaxation necessitated when the alkali ion, OH - ion and so on reciprocate between the adjacent position due to the electric field, (3) distortion loss when the network structure of the glass distorts due to the electric field, and dipole orientation occurs momentarily, and (4) ion vibration loss caused when there is resonance at the proper oscillation frequency decided by the mass of structural ions and the chemical bonding strength of the surroundings. If alkali is substituted with ions that have a large ionic radius such as barium and the like in lossy glass that includes ions with high ionic mobility such as alkali ions, loss can be reduced since the mobility of the ions can be hindered [32, 33, 34].

While dielectric characteristics in the microwave band are determined by ionic polarization and electronic polarization, dielectric loss through electronic polarization is small enough to be ignored, and the following equation can be derived from the one-dimensional lattice vibration model through ionic polarization (qualitatively extensible to three-dimensional ion crystals).

$\tan \delta = (\gamma/\omega_T^2)\ \omega$

ω_T : resonating angular frequency of the optical mode of lattice vibration transverse waves, γ: attenuation constant, ω: angular frequency

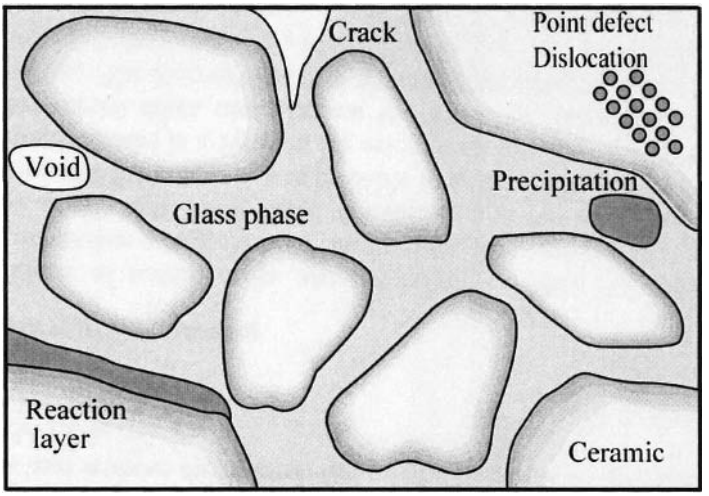

Figure 2-14 Micro and macro defects inherent in LTCCs.

As the presence of lattice defects, impurities and grain boundaries are factors that increase γ, it is effective to use raw materials with high purity to achieve low dielectric loss, and to aim for a microstructure without impurities and without the internal micro and macro flaws that are shown in Figure 2-14 [35].

2.4 Thermal expansion

Several kinds of mixing rules are presented in Table 2-6 regarding the thermal expansion coefficient of composites. By predicting the thermal expansion coefficient using these equations, and by controlling material composition and formulation, it is possible to approach the desired values.

The simple model is a formula for calculating just the mixing ratio, while the Turner model takes into account the effect of isotropic stress of the adjacent phase. The Kerner model is a model that allows for the shear effect of the phase boundary in types with spherical phases distributed isotropically in the matrix, and it shows values between those of the Turner model and the simple model. Table 2-7 shows the calculated values using the Turner model [36, 37], and the actual measurements for glass/ceramic composites using different ceramics. In types where a difference can be seen between the value predicted by the calculation and the actual measurement, precipitation of a secondary crystal phase (cristobalite) is identified. The cristobalites formed when the glass crystallizes in a composite, arise from a phase transition between 100 to 200°C, and thermal expansion changes markedly (refer to Figure 2-15)[38, 39]. Heating at around 200°C is required in the

assembly process of the substrates, and extreme changes in thermal expansion cause connection failures in the interconnects of mounted components that harm the reliability of the product. Figure 2-16 shows the phase formation of the glass phase in a glass/alumina composite when the amount of alumina and the firing temperature are changed. When a little alumina is added and the firing temperature is low, cristobalite crystals are precipitated in the glass phase, and when a lot of alumina is added and the firing temperature is high, mullite crystals are precipitated. In the wide composition and firing temperature range that remains, the glass phase is amorphous, the glass/alumina composite is stable, and cristobalite crystals are suppressed, so it is demonstrated that the thermal expansion coefficient of glass/alumina composites can be controlled. Besides the additives shown in Table 2-7, spinel ($Al_2O_3 \cdot MgO$) containing the ingredient Al_2O_3 has also been identified as an additive that suppresses cristobalite crystals [40].

Table 2-6 Mixture rules for thermal expansion coefficients of composites.

Simple mixture rule	$\alpha = \alpha_1 V_1 + \alpha_2 V_2$
Turner equation	$\alpha = (\alpha_1 V_1 K_1 + \alpha_2 V_2 K_2)/(V_1 K_1 + V_2 K_2)$
Kerner equation	$\alpha = \alpha_1 + V_2(\alpha_1 - \alpha_2) \cdot \{K_1 (3K_2 + 4G_1)^2 + (K_2 - K_1)(16G_1^2 + 12G_1K_2)/(4G_1 + 3K_2)[4V_2G_1(K_2 - K_1) + 3K_2K_1 + 4G_1K_1]$

α_1: thermal expansion coefficient of constituent material 1, α_2: thermal expansion coefficient of constituent material 2, V_1: volume fraction of constituent material 1, V_2: volume fraction of constituent material 2, K_1: volume modulus of constituent material 1, K_2: volume modulus of constituent material 2, G: shear modulus

Table 2-7 Thermal expansion coefficients ($\times 10^{-6}$/°C) of each type of glass/ceramic composite (Calculated value using Turner equation and the actual measurement).

Material type	Calculated value	Measured value
Alumina (Al_2O_3) - glass	4.6	4.0
Aluminum nitride (AlN) - glass	3.6	3.5
Mullite ($3Al_2O_3 \cdot 2SiO_2$) - glass	4.8	3.9
Forsterite ($2MgO \cdot SiO_2$) - glass	5.7	18.2
Steatite ($MgO \cdot SiO_2$) - glass	4.6	17.4
Magnesium oxide (MgO) - glass	5.7	18.3
Silicon nitride (Si_3N_4) - glass	3.1	17.1

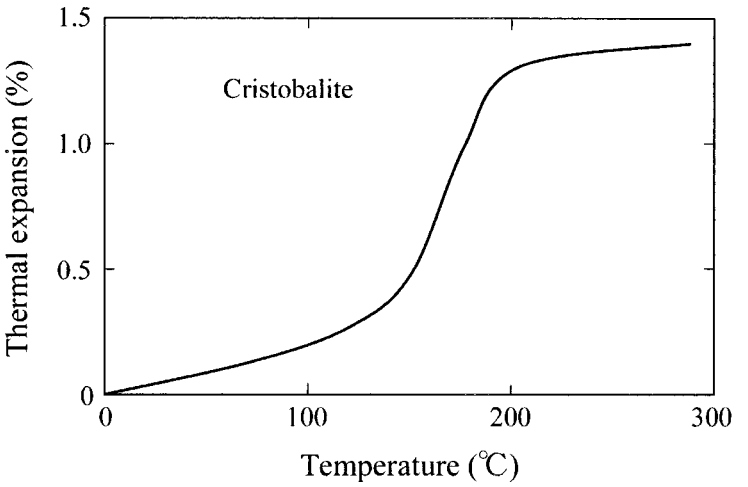

Figure 2-15 Cristobalite thermal expansion curve.

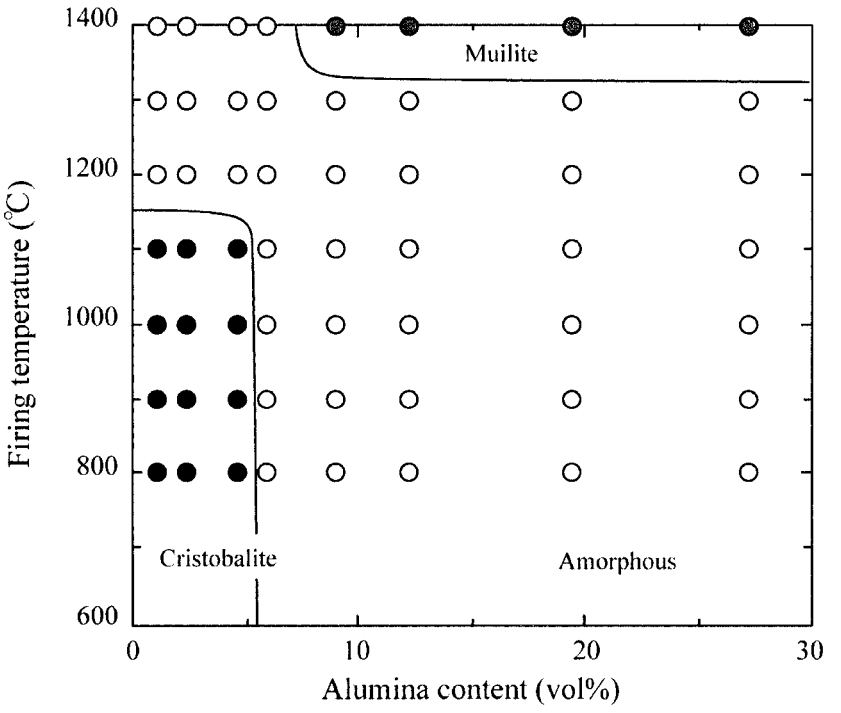

Figure 2-16 Phase formation when the composition and firing temperature of glass/alumina composite are taken as the parameters.

2.5 Mechanical strength

In glass/ceramic composites with distributed ceramic particles, mechanical strength varies according to (1) composition (amount of ceramic), (2) porosity, and (3) ceramic particle diameter. Figure 2-17 shows the flexural strength of a glass/alumina composite when each parameter is changed. In cases where the composition (amount of ceramic) is the parameter, in accordance with the simple mixing rule, strength is seen to improve along with the increase in the amount of alumina [41]. The relationship between porosity and strength nearly fits the following equation proposed by Ryskewitsch, and strength can be predicted using this equation; $\sigma = \sigma_0 \cdot \exp(-np)$, (n: constant, p: porosity) [42]. The flexural strength of glass/ceramic composites when the dispersed particle diameter (d) is varied closely matches the Orowan and Hall-Petch relationship ($\sigma \propto d^{1/2}$) [43, 44], and stronger ceramic can be achieved with the use of alumina with a fine particle diameter. The strength achieved by using finer ceramic particles in glass/ceramic composites is due to their ability to spend the energy required to transmit cracks by dissipating cracks that occur and making them zigzag (boarding and deflection of cracks) (refer to Figure 2-18). With the following management of parameters, it is possible to control the strength of the glass/ceramic composite itself.

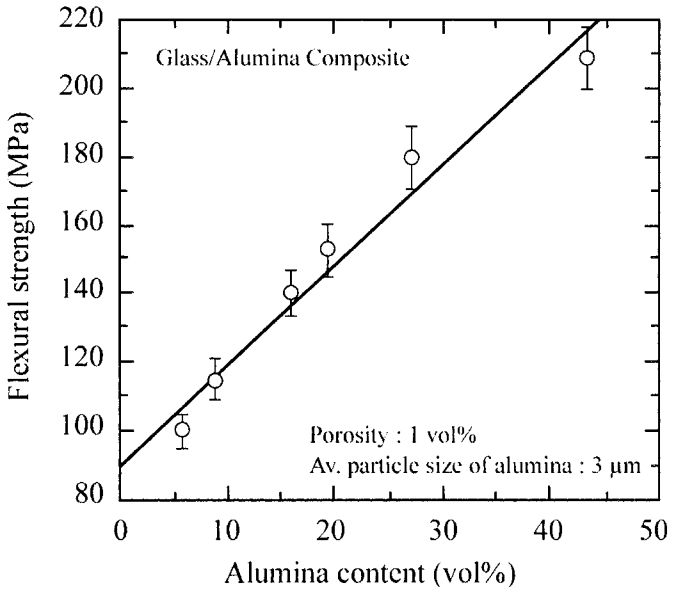

(a)

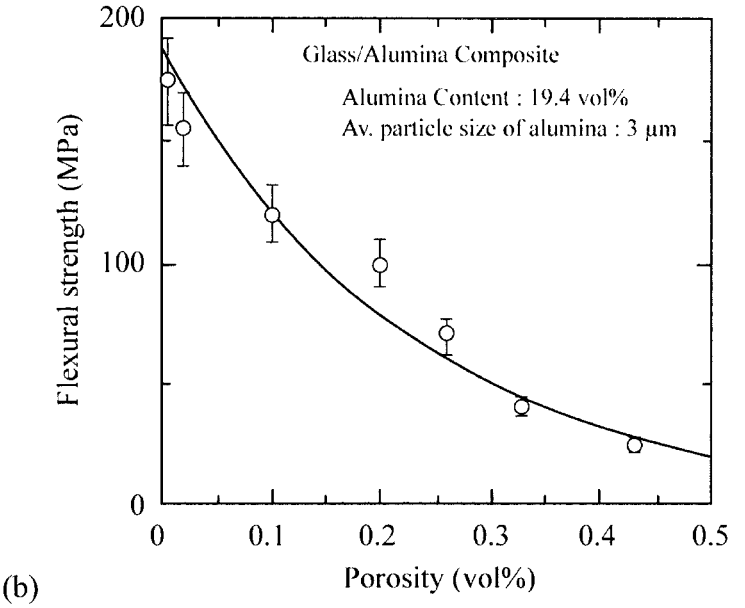

(b)

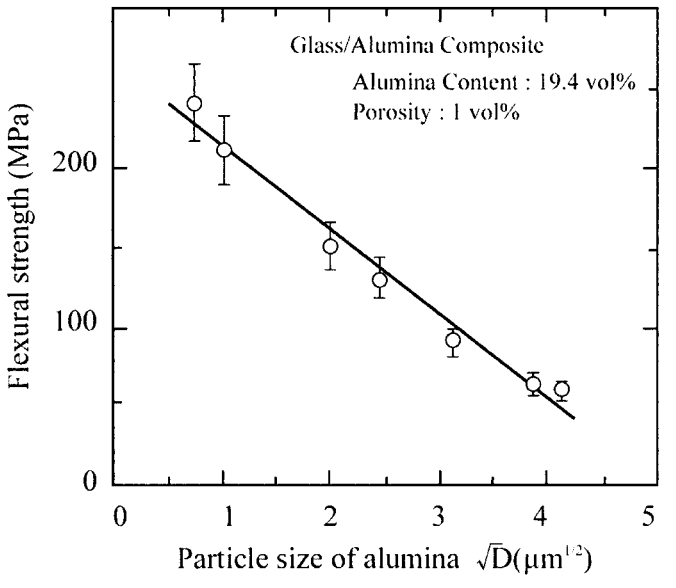

(c)

Figure 2-17 Flexural strength of glass/alumina composite when (a) composition (amount of ceramic), (b) porosity, and (c) dispersed particle diameter are varied.

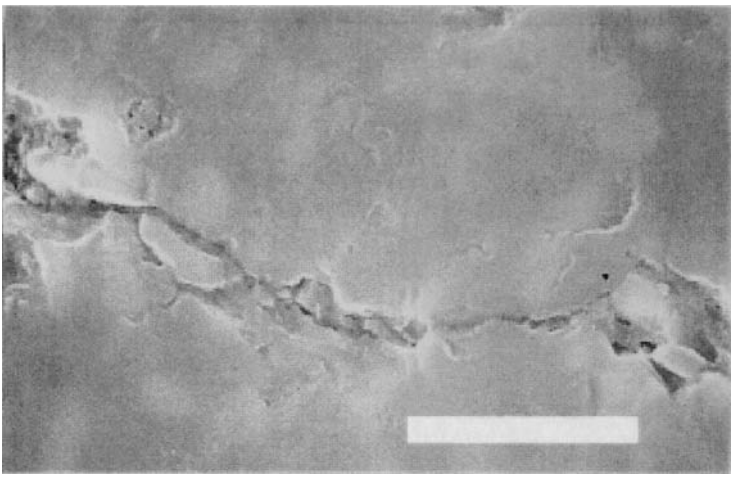

Figure 2-18 Transmission of cracks in glass/alumina composite [Bar = 10 μm].

2.5.1 Strengthening the glass phase

Strengthening a weak glass phase is effective in order to strengthen glass/ceramic composites. The following two methods are known to strengthen the glass phase. (1) Crystallized glass method, and (2) ion exchange strengthening method

With the crystallized glass method, crystals with low thermal expansion formed due to compressive stress are precipitated in the amorphous glass matrix. There are two methods, one using glass material that crystallizes readily, and the other by precipitating crystals by promoting a reaction between the alumina and glass during the firing process.

In the ion exchange strengthening method as shown in Table 2-8, the glass is immersed in molten salt containing potassium ions, and by introducing larger potassium ions into the surface of the glass in place of the sodium ions, the glass network expands, resulting in increased strength due to the compressive stress created (refer to Figure 2-19 for the strength principle) [45, 46]. When borosilicate glass/alumina composite is immersed for 30 hours in KNO_3 at 400°C, as shown in Figure 2-20, it is found that potassium penetrates the surface to a depth of around 100 μm, and bending strength is improved by more than 50% (non-treated: 150 MPa, after ion exchange: 230 MPa).

Variation in the strength of ceramic occurs readily and to evaluate this variation, the Weibull modulus is frequently applied. The Weibull modulus is found as follows.

The relationship between the failure probability P_s of all samples and stress σ when they break is as follows [47].

$P_s = \exp[- V((\sigma - \sigma_u)/\sigma_0)^m]$
σ_u: Stress at which breakage does not occur (usually 0)
σ_0: Normalization constant
m: Weibull modulus

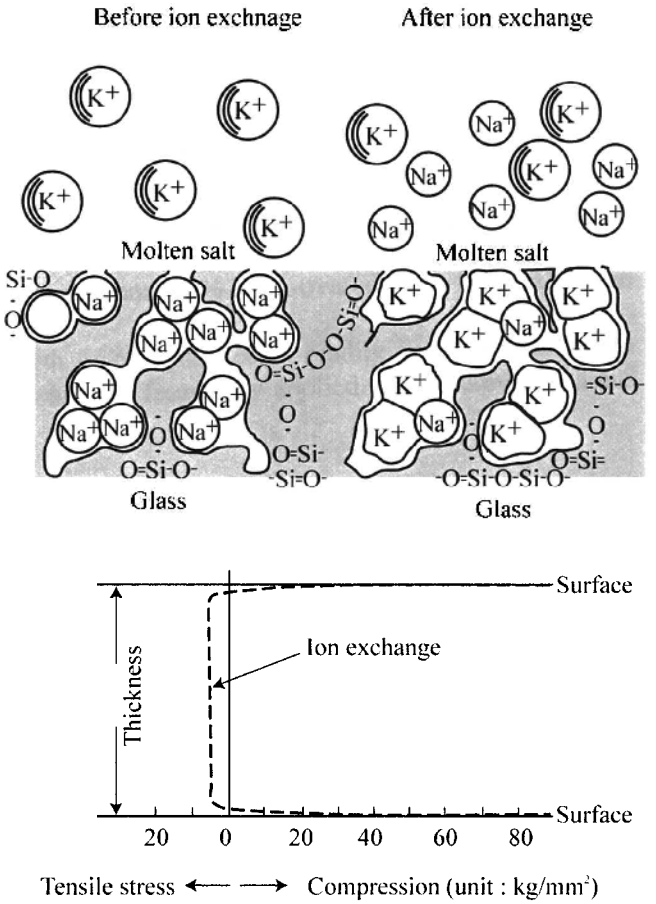

Figure 2-19 Principle of strengthening of the glass due to $Na^+ \rightarrow K^+$ exchange.

If we take the double logarithm of the above equation,
$\ln\ln(1/ P_s) = \ln V + m\ln(\sigma - \sigma_u) - m\ln \sigma_0$
By plotting the equation on a Weibull modulus sheet and finding the gradient of the straight line, the Weibull modulus can be found. The

measured strength values around N for all samples are arranged from the highest value, and breaking at i is defined as P_s = 1-i/(N+1). Materials with a big Weibull modulus (a big gradient on the Weibull plot) have little variation in strength.

Table 2-8 Physical properties of various kinds of potassium salt.

Potassium salt	K content (%)	Melting point (°C)	Water solution
KNO_3	83	330	Neutral
KCl	52	776	Neutral
K_2SO_4	65	1, 067	Neutral
K_3PO_4	55	1, 340	Alkaline
K_2HPO_4	45	807	Alkaline
K_2CO_3	57	891	Alkaline
KOH	70	360	Alkaline

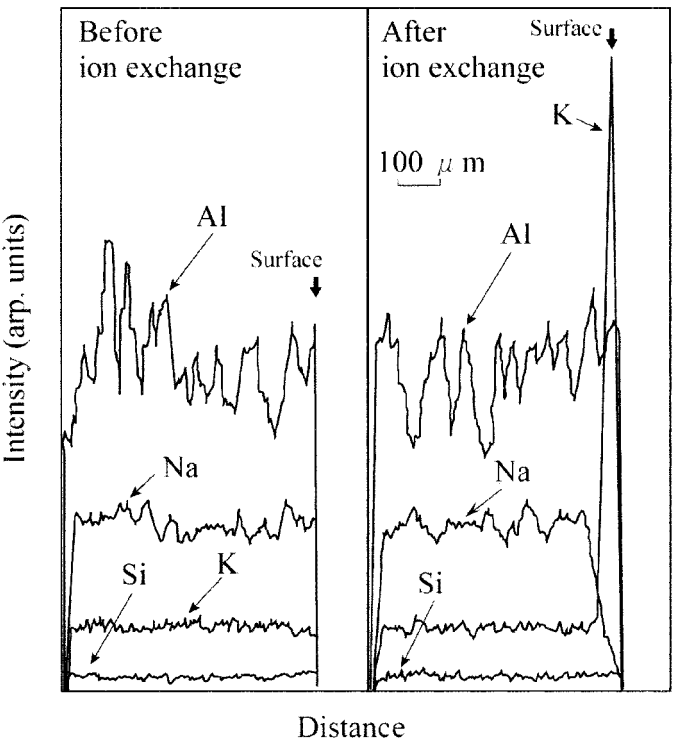

Figure 2-20 EPMA results of a cross section of glass/alumina composite before and after ion exchange treatment (immersion in KNO_3 at 400°C for 30 h).

With device level LTCCs, the glass/ceramic composites themselves are not used separately, but are formed with conductor wiring in each layer and via conductors between layers. Seen from a macro point of view, they can be characterized as composite materials formed of wiring metal and ceramic. For this reason, in order to improve the strength of the LTCC overall, it is effective to reduce micro and macro flaws in the metal/ceramic interface, and to predict and improve strength, with reference to the equation suggested with fiber reinforced resin material below [48].

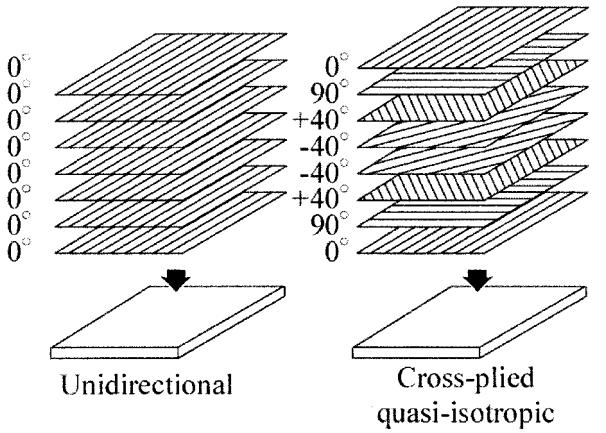

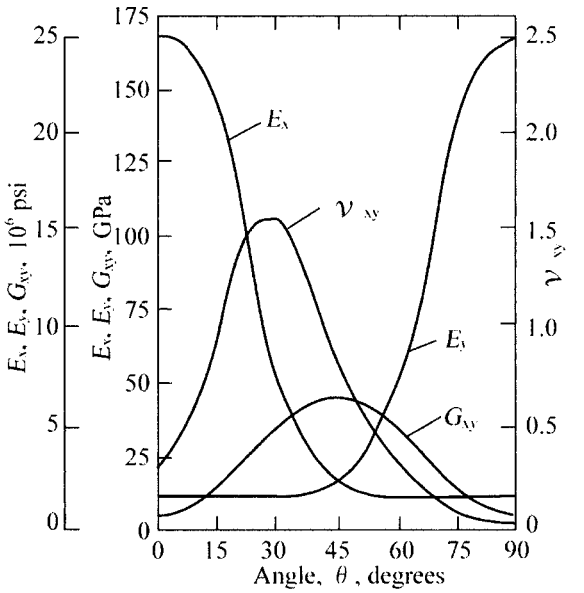

Figure 2-21 The various changes in mechanical properties when the arrangement angle of carbon fibers in an epoxy/carbon fiber composite laminate is varied.

$E_c = E_f V_f + E_m(1 - V_f)$ (for constraint strain)
$1/E_c = V_f/E_f + (1 - V_f)/E_m$ (for constraint stress)
E_c: modulus of composite, E_f: modulus of fiber, E_m: modulus of matrix, V_f: fiber volume fraction

Figure 2-21 shows an example where the arrangement angle of carbon fibers in an epoxy/carbon fiber composite laminate is varied in order to change its mechanical properties when laminated. However, if we consider the use of the LTCC wiring in place of the carbon fibers, the mechanical properties of the whole LTCC can be improved by arranging the wiring at an angle. However, there are problems with screen printing diagonal wiring and further process technology development is required for its application.

2.5.2 Thermal shock resistance

When heating a material, the thermal expansion of the high temperature side is greater than that of the low temperature side, and the compressive stress of the heated surface pulls on the inside of the material on the low temperature side causing stress. Conversely, when cooling, the pull is towards the surface causing stress. In this way, when heating and cooling materials, thermal stress (compressive and tensile stress) occurs. Since the compressive strength of ceramics is markedly greater when compared with their tensile strength, cracks start in the weakest parts of those parts where tensile stress is present. The thermal shock resistance coefficient, which is the index for thermal stress σ and thermal shock resistance, is expressed with the following equation [49, 50].

$\sigma = (E\alpha\Delta T)/(1 - \mu)$
μ: Poisson's ratio, E: elastic modulus, ΔT: temperature difference $(T - T_0)$
α: thermal expansion coefficient

With regard to the thermal shock of abrupt cooling from a high temperature, the temperature difference between the initial temperature and the temperature at which cracks start forming in the material ΔT_{max} is called the thermal shock resistance coefficient, and the higher this value, the stronger the resistance to shock.

$\Delta T_{max} = R = \sigma_f(1 - \mu)/ E\alpha$
σ_f: fracture strength,

When heating and cooling is slow, thermal conductivity k is added, and thermal shock resistance is defined as R'.

$$R' = \sigma_f(1 - \mu)k/(E\alpha)$$

Furthermore, if heating and cooling is performed at a certain speed, and thermal diffusivity ($\delta = k/\rho C$) is inserted, thermal shock resistance R" is defined with the following equation.

$$R'' = \sigma_f(1 - \mu)(k/\rho C)/(E\alpha) = R'/(\rho C)$$

Table 2-9 Physical properties of thermal shock resistance of LTCCs and their constituent materials.

	Glass/alumina composite	Alumina	Borosilicate glass (Pyrex)
Young's modulus E ($\times 10^6$ MPa)	0.093	0.38	0.07
Poisson's ratio μ	0.17	0.24	0.16
Thermal expansion coefficient α ($\times 10^{-6}$/°C)	4.1	8.0	3.0
Fracture strength σ_f (MPa)	150	300	80
Thermal shock resistance R	326	75	320
Fracture critical temperature T_{max} (°C)	500	200~300	--
Thermal conductivity k (W/mK)	2.5	16	0.96

Table 2-9 shows the related physical properties of thermal shock resistance of LTCCs and their constituent materials, while Figure 2-22 shows fracture strength of a glass/alumina composite after thermal shock is applied at various temperature differences, and its material microstructure after breaking. As shown in Table 2-9, the thermal shock resistance of glass/alumina composites is greater than that of alumina, and it has excellent reliability with regard to the heat history undergone during the various kinds of assembly.

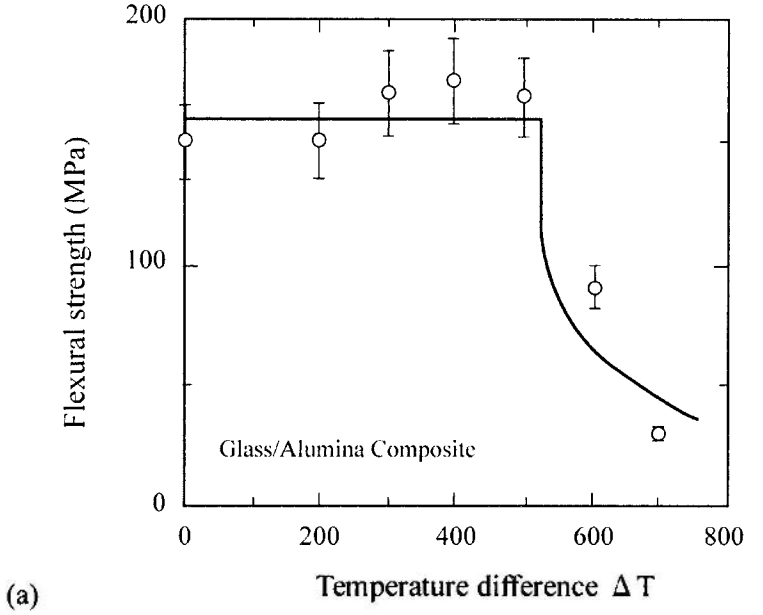

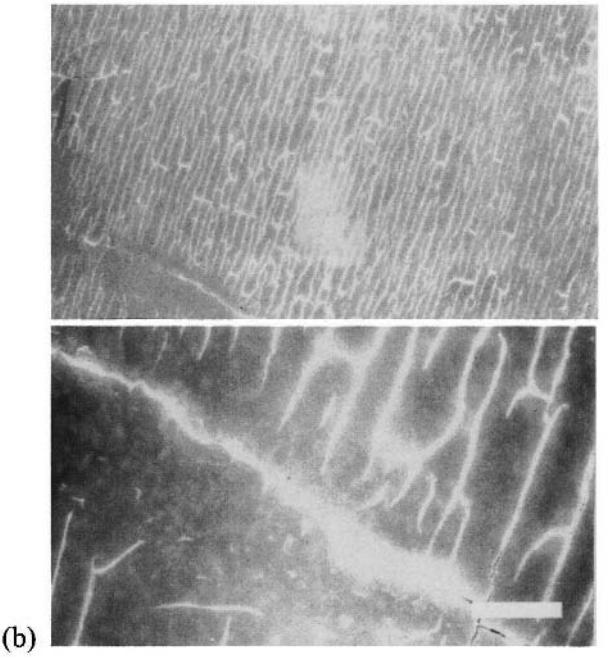

Figure 2-22 Thermal shock resistance of glass/alumina composite (a), and material microstructure after thermal shock fracture (b)
[Bar = 20μm].

2.6 Thermal conductivity

The mixture rule for thermal conductivity normally applied for composite materials is shown below [51].

$k = V_1k_1 + V_2k_2$ ..... (2-7)

$1/k = V_1/k_1 + V_2/k_2$ ..... (2-8)

$\log k = V_1\log k_1 + V_2\log k_2$ ..... (2-9)

k: thermal conductivity of the composite material, k_1: thermal conductivity of constituent material 1, k_2: thermal conductivity of constituent material 2, V_1: volume fraction of constituent material 1, V_2 : volume fraction of constituent material 2

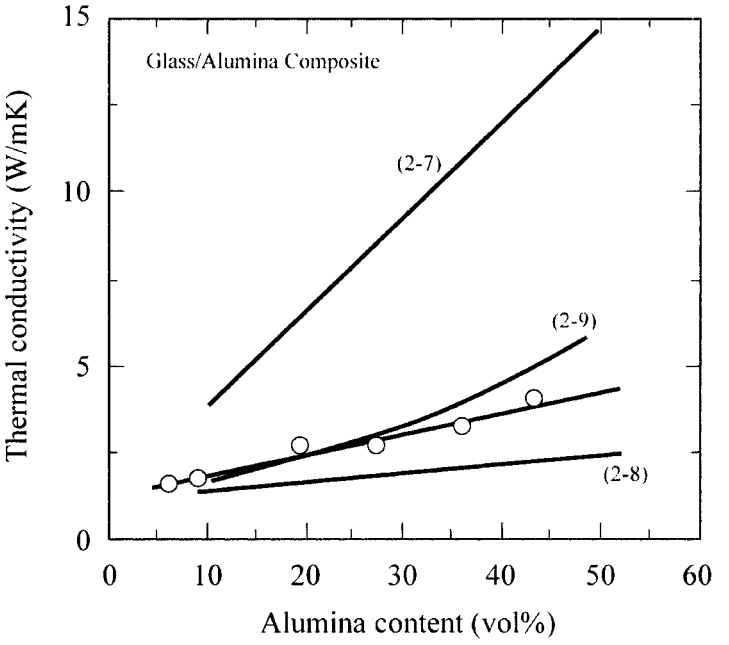

Figure 2-23 Thermal conductivity of glass/alumina composite (actual measurement and calculated value). The numbers in the Figure correspond to the formula numbers.

Equation (2-7) is the mixing rule when heat flow speed direction and the constituent materials are arranged in parallel, and equation (2-8) is when

heat flow speed direction and constituent materials are arranged perpendicularly. Glass/ceramic composites of the type in which ceramic particles are distributed in a glass matrix make a good match with the empirical logarithmic law displaying intermediate values of both. Figure 2-23 shows the actual measurement and the values applied to these formulae for a borosilicate glass/alumina composite. When the thermal conductivity of the alumina and borosilicate glass are 28 W/mK and 1.3 W/mK respectively, the thermal conductivity of the glass/alumina composite with alumina content of 19.4 vol% is 2.7 W/mK, and this shows a good approximation to the calculated value of 2.4 W/mk using the logarithmic law.

In order to achieve high thermal conductance, aluminum nitride, silicon nitride, silicon carbide and the like which have high thermal conductance are being tried as ceramic ingredients. However whatever the type, it is difficult to exceed that of the alumina used in HTCCs. However, compared with resin materials, glass/alumina composites can achieve thermal conductivity more than ten times higher.

References

[1] N. Kamehara, Y. Imanaka, and K. Niwa, "Multilayer Ceramic Circuit Board with Copper Conductor", Denshi Tokyo, No. 26, (1987), pp. 143-148.

[2] R. R. Tummala et al., "High performance glass-ceramic/copper multilayer substrate with thin-film redistribution", IBM J. Res. Develop., Vol. 36, No. 5 Sep. (1992), pp. 889-904.

[3] System Design: Say good-bye to PCI, say hello to serial interface, NIKKEI ELECTRONICS, 2001. 6. 18., no. 798 , pp. 119.

[4] Y. Usui, "Quantitative Analysis Overcomes Design Bottleneck for PCB's with Speeds over 1GHz", NIKKEI ELECTRONICS, 2002. 1. 7, pp. 107-113.

[5] A. A. Mohammed, "LTCC for High-Power RF Application?", ADVANCED PACKAGING, Oct. (1999), pp. 46-50.

[6] D. I. Amey, M. T. Dirks, R. R. Draudt, S. J. Horowitz, and C. R. S. Needs, "Opening the door to wireless innovations", ADVANCED PACKAGING, Mar. (2000) , pp. 37-540.

[7] T. Hayashi, T. Inoue, and Y. Akiyama, "Low-Temperature Sintering and Properties of (Pb, Ba, Sr)(Zr, Ti, Sb)O_3 Piezoelectric Ceramics Using Sintering Aids", Jpn. J. Appl. Phys. Vol. 38, (1999), pp. 5549-5552.

[8] K. Murakami, D. Mabuchi, T. Kurita, Y. Niwa, and S. Kaneko, "Effects of Adding Various Metal Oxides on Low-Temperature Sintered Pb(Zr, Ti)O_3 Ceramics", Jpn. J. Appl. Phys. Vol. 35, (1996), pp. 5188-5191.

[9] W. A. Schulze and J. V. Biggers, "Piezoelectric Properties of $Pb_5Ge_3O_{11}$ Bonded PZT Compositions", Mat. Res. Bull., 14, (1979), pp. 721-30.

[10] J. H. Jean and T. K. Gupta, "Isothermal and Nonisothermal Sintering Kinetics of Glass-Filled Ceramics", J. Mater. Res., Vol. 7, No. 12, (1992), pp. 3342-48.

[11] C. R. Chang and J. H. Jean, "Camber Development during Cofiring an Ag-based Ceramic-Filled Glass Package", Ceramic Transactions Vol. 97, (1999), pp. 227-239.

[12] G. C. Kuczynski and I. Zaplatynskyj, "Sintering of Glass", J. Am. Ceram. Soc. , Vol. 39, No. 10, (1956), pp. 349-350.

[13] I. B. Cutler and R. E. Henrichsen, "Effect of Particle Shape on the Kinetics of Sintering of Glass", J. Am. Ceram. Soc. , Vol. 51, No. 10, (1968) pp. 604-05.

[14] W. J. Zachariasen, J. Am. Ceram. Soc., Vol. 54, (1932) pp. 3841.

[15] Corning , "The Characterization of Glass and Glass-Ceramics"

[16] D. Clinton, R. A. Marcel, R. P. Miller, J. Material Science, Vol. 5, (1970), pp. 171.

[17] J. Frenkel, Kinetic Theory of Liquids, Oxford University Press, (1946) pp. 424.

[18] X. Zhou and M. Yamane, "Effect of Heat-Treatment for Nucleation on the Crystallization of MgO-Al_2O_3-SiO_2 Glass Containing TiO_2", J. Ceram. Soc. of Jpn, Vol. 96, No. 2, (1988), pp. 152-588.

[19] J. H. Jean and T. K. Gupta, "Crystallization kinetics of binary borosilicate glass composite", J. Mater. Res., Vol. 7, No. 11, (1992), pp. 3103-3111.

[20] J. H. Jean and T. K. Gupta, "Devitrification inhibitors in borosilicate glass and binary borosilicate glass composite", J. Mater. Res., Vol. 10, No.5, (1995), pp. 1312-1320.

[21] Y. Imanaka, N. Kamehara, and K. Niwa, "The Sintering Process of Glass/Alumina Composites", J. Ceram. Soc. of Jpn, Vol. 98, No. 8, (1990), pp. 812-816.

[22] H. Jebsen-Marwedel, Glastechn. Ber., Vol. 20, (1942) pp. 221.

[23] J. Loeffler, Glastechn. Ber., Vol. 23, (1950), pp. 11.

[24] H. Jebsen-Marwedel, Glastechn. Ber., Vol. 25, (1952), pp. 119.

[25] J. Widtmann, Glastechn. Ber., Vol. 29, (1956), pp. 37.

[26] Y. Imanaka, S. Aoki, N. Kamehara, and K. Niwa, "Crystallization of Low Temperature Fired Glass/Ceramic Composite", J. Ceram. Soc. of Jpn, Vol. 95, No. 11, (1987), pp. 1119-1121.

[27] Y. Imanaka, K. Yamazaki, S. Aoki, N. Kamehara, and K. Niwa, "Effect of Alumina Addition on Crystallization of Borosilicate Glass", J. Ceram. Soc. of Jpn, Vol. 97, No. 3, (1989), pp. 309-313.

[28] S. Nishigaki, S. Yano, J. Fukuta, M. Fukaya and T. Fuwa, "A NEW MULTILAYERED, LOW-TEMPERATURE-FIREABLE CERAMIC SUBSTRATE", Proceedings '85 International Symposium of Hybrid Microelectronics (ISHM), (1985), pp. 225-34.

[29] S. Wahisa, The Journal of Electronics and Communication Engineers of Japan, Vol 49, No. 7, (1966), pp. 37-47.

[30] N. Yamaoka, M. Masaru and M. Fukui, Am. Ceram. Soc. Bull., Vol. 62, No. 6, (1983) pp. 698.

[31] W. D. Kingery, H. K. Bowen and D. R. Uhlmann: Introduction to Ceramics (John Wiley & Sons, Inc., 1976).

[32] P. M. Sutton, "Dielectric Properties of Glass", Briks & Schulman Progress in Dielectrics II, (1960) pp. 114-161.

[33] V. Hippel, "Dielectric Materials and Its Application"

[34] V. D. Frechette, "Non-Crystalline Solids", (1960), pp. 412.

[35] Y. Imanaka, "Material Technology of LTCC for High Frequency Application", Material Integration, Vol. 15, No. 12 (2002), pp. 44-48.

[36] R. R. Tummala and A. L. Friedgerg, "Composites, Carbides-Thermal Expansion of Composite Materials", J. Appl. Phys., Vol. 41, No. 13, (1970), pp. 5104-5107.

[37] P. S. Turner, J. Res. NBS, Vol. 37, (1946), pp. 239.

[38] H. M. Kraner, Phase Diagrams, Material Science and Technology, 6-II, (1970), pp. 83-87.

[39] C. N. Fenner, J. Am. Ceram. Soc., Vol. 36, (1913), pp. 331-384.

[40] Y. Imanaka, S. Aoki, N. Kamehara, and K. Niwa, "Cristobalite Phase Formation in Glass/Ceramic Composites", J. Am. Ceram. Soc. Vol. 78, No. 5, (1995), pp. 1265-1271.

[41] Y. Imanaka, "Multilayer Ceramic Substrate, Subject and Solution of Manufacturing Process of Ceramics for Microwave Electronic Component", Technical Information Institute, (2002), pp. 235-249.

[42] Ryskewitsch, "Compression Strength of Porous Sintered Alumina and Zirconia", J. Am. Ceram. Soc., Vol. 36, No. 2, (1953), pp. 65-68.

[43] E. Orowan, "Fracture and Strength of Solids [Metals]", Repts. Progr. in Phys., Vol. 12, (1949), pp. 185-232.

[44] N. J. Petch, "Cleavage Strength of Polycrystals", J. Iron Steel Inst. (London), 174, Part I, May, (1953), pp. 25-28.

[45] S. Kistler, J. Am. Ceram. Soc., Vol. 45, No. 2, (1962), pp. 59.

[46] M. Nordberg, E. Mochel, H. Garfinkel, J. Olcott, J. Am. Ceram. Soc., Vol. 47, (1964) pp. 215.

[47] W. Weibull, "A Statistical Distribution Function of Wide Applicability", J. Appl. Mech. Vol. 18, (1951), pp. 293.

[48] R. M. Jones, Mechanics of Composite Materials, McGraw Hill, New York (1975).

[49] R. W. Davidge and G. Tappin, "Thermal Shock and Fracture in Ceramics", Trans. Br. Ceram. Soc. Vol. 66, (1967) pp. 405.

[50] D. P. H. Hasselman, Unified Theory of Thermal Shock Fracture Initiation and Crack Propagation in Brittle Ceramics, J. Am. Ceram. Soc. Vol. 49, (1969), pp. 68.

[51] W. D. Kingery, H. K. Bowen and D. R. Uhlmann: Introduction to Ceramics 2nd ed. (John Wiley & Sons, Inc., (1976), pp. 634.

http://www.springer.com/978-0-387-23130-3

Multilayered Low Temperature Cofired Ceramics (LTCC) Technology

Imanaka, Y.

2005, XXXI, 229 p., Hardcover
ISBN: 978-0-387-23130-3